

2025

# Fragmentation characteristics of long bones resulting from impact of different ammunition sizes

---

<https://hdl.handle.net/2144/52316>

*"Downloaded from OpenBU. Boston University's institutional repository."*

BOSTON UNIVERSITY

ARAM V. CHOBANIAN & EDWARD AVEDISIAN SCHOOL OF MEDICINE

Thesis

**FRAGMENTATION CHARACTERISTICS OF LONG BONES RESULTING  
FROM IMPACT OF DIFFERENT AMMUNITION SIZES**

by

**JULIA MCGOWAN**

B.A., George Mason University, 2023

Submitted in partial fulfillment of the  
requirements for the degree of

Master of Science

2025

© 2025 by  
JULIA MCGOWAN  
All rights reserved

Approved by

First Reader

---

James Pokines, Ph.D.  
Associate Professor of Anatomy and Neurobiology

Second Reader

---

Tara L. Moore, Ph.D.  
Professor of Anatomy and Neurobiology

## **ACKNOWLEDGMENTS**

Thank you to Dr. James T. Pokines and Dr. Tara L. Moore for all their assistance in facilitating this project. To the Boston University Anatomy and Forensic Anthropology Departments, thank you for the funding and allowing me the use of facilities that made this project possible. Thank you, also, to the members of the Massachusetts Federal Law Enforcement for allowing me use of the Fort Devens Shooting Range and their participation in my research.

I would also like to acknowledge my parents, fiancé, and classmates for their continued support of my project and helping me persevere through these two years of graduate school.

**FRAGMENTATION CHARACTERISTICS OF LONG BONES RESULTING  
FROM IMPACT OF DIFFERENT AMMUNITION SIZES**

**JULIA MCGOWAN**

**ABSTRACT**

The present study examined differences in fragmentation and trauma characteristics on long bones caused by two ammunition types. White-tailed deer (*Odocoileus virginianus*) tibiae (n = 50) were encased in 10% ballistic gelatin, and 9 mm ammunition from a handgun and 5.56 mm ammunition from an assault rifle were fired from a distance of 3 yards. Due to the higher muzzle velocity, it is anticipated that tibiae impacted by 5.56mm ammunition will exhibit a greater degree of fragmentation and obscure fracture patterns. Conversely, fragmentation patterns from 9 mm ammunition are expected to be more discernible, given the lower energy transfer and smaller caliber, allowing for easier classification of fracture patterns including drill-hole, impaction and false butterfly. A Kolmogorov-Smirnov test indicated the number of fragments for each ammunition type followed a normal distribution ( $Df(25) = 0.139$ ,  $p = 0.200$ ) for 9 mm and ( $Df(25) = 0.090$ ,  $p = 0.200$ ) for 5.56 mm ammunition. A Mann-Whitney U-test revealed 5.56 mm ammunition caused more fragmentation than 9 mm ( $p = 0.002$ ). Of the examined-for fracture patterns, only false butterfly fractures were observed, in 48% of the 9 mm sample and 4% of the 5.56 mm sample. Chi-square tests for independence showed that all but stepped breakout ( $\chi^2(1) = 1.299$ ,  $p = 0.254$ ) had a statistical association with an ammunition type. The present study found significant differences between the frequency of observed ballistic characteristics and ammunition type offering a potential

method for identifying ammunition types in future cases of ballistic trauma where no projectile is present.

**TABLE OF CONTENTS**

ACKNOWLEDGMENTS ..... iv

ABSTRACT ..... v

TABLE OF CONTENTS..... vii

LIST OF TABLES ..... ix

LIST OF FIGURES ..... x

LIST OF ABBREVIATIONS..... xii

INTRODUCTION ..... 1

    Firearm Violence and Ballistic Research..... 1

    Evidence Criteria – Daubert Standard ..... 3

    Rationale and Hypothesis ..... 4

PREVIOUS RESEARCH..... 6

    Ballistic Fracture Patterns ..... 6

    Model for Ballistic Trauma..... 6

METHODS ..... 10

    Materials ..... 10

    Data Collection and Statistics ..... 11

RESULTS ..... 14

DISCUSSION ..... 17

CONCLUSIONS..... 22

BIBLIOGRAPHY ..... 34

CURRICULUM VITAE..... 41

## LIST OF TABLES

Table	Title	Page
1	Fragmentation of 9 mm and 5.56 mm samples	33
2	Observed characteristics of ballistic trauma based upon ammunition.	33

## LIST OF FIGURES

Figure	Title	Page
1	Two deer tibiae are embedded in 10 cm of ballistic gelatin. The anterior aspects are approximately 5 cm below the surface. There is an aluminum divider between the two tibiae, so they can each be impacted separately.	23
2	Anterior aspect of tibia impacted by 5.56 mm ammunition. The entry and exit wounds are heavily comminuted, irregular, and largely indistinguishable from each other. Long oblique fracture lines run along the diaphysis toward the far proximal and distal extremities. The scale is in cm.	24
3	Anterior aspect of tibia impacted by 9 mm ammunition. The entry wound is round with radiating and concentric fractures. Internal beveling is present. Bullet wipe (arrows) is evident along the margins of the entry wound. The scale is in cm.	25
4	Postero-distal portion of tibia impacted by 5.56 mm ammunition. Layered concentric fractures (arrows) on the posterior surface are created by a stepped breakout fracture pattern. Stepped breakout pattern is distinguishable by the similar shaped fragments. The scale is in cm.	26
5	Antero-proximal portion of tibia impacted by 5.56 mm ammunition. The impact created a long radiating fracture that split the diaphysis in half. The scale is in cm.	27
6	Distal portion of tibia impacted by 5.56 mm ammunition. A long, oblique radiating fracture line runs distally down the diaphysis. The scale is in cm.	28
7	Anterior aspect of tibia impacted by 9 mm ammunition. The entry wound is rounded with radiating linear fractures. Pattern formed by impact is a false butterfly fracture. The scale is in cm.	29
8	Anterior aspect of tibia impacted with 9 mm ammunition. The entry wound is round, with internal beveling and small specks of bullet wipe along the margins. A false butterfly fracture pattern is created by the four prominent fracture lines radiating from the entry wound. The scale is in cm.	30

- 9            Posterior aspect of tibia impacted by 9 mm ammunition. Entry wound is round and exit wound is irregular and more comminuted. Fracture margins are jagged and no external beveling could be observed around the exit wound. Posterior aspect shows stepped breakout consisting of radiating and concentric fractures. The scale is in cm.            31

**LIST OF ABBREVIATIONS**

- FMJ ..... Full metal jacket
- FPS ..... Feet per second
- GSW ..... Gunshot wound
- JHP ..... Jacketed hollow point

## INTRODUCTION

### **Firearm Violence and Ballistic Research**

In recent decades, firearm violence has become increasingly prevalent both nationally and internationally (Dougherty et al. 2009). In the United States alone, approximately 70,000 nonfatal gunshot injuries occur each year (Su et al. 2018). Between 2006 and 2010, firearm-related injuries led to 385,769 emergency room visits, 141,914 hospital admissions, and an economic burden of \$88.6 billion in the U.S. (Su et al. 2018). By 2020, firearm-related incidents surpassed motor vehicle accidents as the leading cause of death among children and teenagers, with homicides being the most common type of incident in the U.S. (Brownlee 2023). In 2023, there were 36,357 firearm injuries and 18,874 firearm-related deaths, excluding suicides (Brownlee 2023). Despite the growing number of gunshot injuries, research on ballistic bone trauma has remained limited, particularly in understanding the impact patterns of gunshot wounds (GSW) to long bones. Most research on ballistic trauma has focused on flat bones, such as the cranium, which are more commonly associated with fatal injuries (Berryman 2019; Hart 2005; Humphrey et al. 2017; Ross 1996; Smith et al. 1987). In many cases of gunshot violence, however, the extremities are also impacted (Watson et al. 2023). There is a clear need for further investigation into the fracture patterns of long bones from different projectiles to improve our understanding of ballistic trauma and assist in forensic reconstructions, especially when the type of projectile is unknown.

As firearm violence continues to rise, it is essential for medical and forensic professionals to become well-versed in fracture and wound analysis. Flieger et al. (2016)

found that in a sample of 897 homicide cases from the Institute of Legal Medicine in Frankfurt, 70.9% of victims had at least one bony injury, 45.5% had multiple bony injuries, and 92.6% of total gunshot victims sustained bony injuries. Similarly, Maiden et al. (2016) reported that in a study of 197 homicide cases from the National Centre of Forensic Medicine in Tel Aviv, Israel, ribs were injured in 328 out of 440 instances of GSW to the thorax and abdomen, or nearly 75% of the cases.

The U.S. temporarily imposed a ban on military assault weapons in 1994, but this restriction expired in 2004 (Koper, 2004). Perpetrators of crime often perceive automatic weapons as more powerful, and large-capacity magazines (LCMs) allow more bullets to be fired before reloading. Handguns are even more prevalent in firearm-related incidents. Hawes et al. (2016) reported that in 1,081 cases of violent death due to gunshot injuries in Shelby County and Davidson County, Tennessee between 2009 and 2012, handguns were involved in 83% of the cases. Homicide was the most common cause of death, accounting for 61% of the cases. Rickman and Smith (2014) noted that handguns were responsible for up to 90% of conflict deaths, 40% of homicides, and 6% of suicides in Brazil and Colombia in 2003. The most common handgun cartridge worldwide is the 9 mm full metal-jacket (Sexton et al. 2024). The present study focuses on 9 mm and 5.56 mm ammunition, which are both widely accessible and associated with commonly used firearms.

### **Evidence Criteria – Daubert Standard**

Before the Daubert Standard was introduced in 1993 through the Supreme Court case *Daubert v. Merrell Dow Pharmaceuticals*, courts often relied on forensic evidence

presented by recognized experts. These individuals were valued primarily for their academic qualifications and years of experience, rather than the scientific rigor of their methods (Dirkmaat et al. 2008). The previous standard, known as the Frye Standard, originated from *Frye v. United States* in 1923. Under this rule, evidence could be presented if it was generally accepted within the relevant scientific community (Cheng and Yoon 2005). In some specialized fields, experts often maintained unique standards and practices that did not necessarily align with broader scientific consensus (Fienberg et al. 1995). Recognizing this issue, the Supreme Court ruled in *Daubert v. Merrell Dow Pharmaceuticals* that general acceptance alone wasn't a sufficient basis for admitting scientific evidence in court. Instead, they established the Daubert Standard, which prioritizes testable, replicable, reliable, and scientifically validated methods (Dirkmaat et al. 2008).

To prevent unreliable or pseudoscientific claims from influencing legal decisions, the Daubert Standard relies on four key criteria: testability, peer review and publication, error rate, and general acceptance (Fournier 2016). Testability ensures that an expert's methods and claims can be objectively assessed using the scientific method. Peer review and publication reflect the scientific community's evaluation of a method's validity and reliability. Error rate refers to the likelihood of mistakes within a particular method and the significance of those errors in drawing conclusions. Finally, while general acceptance remains a factor under the Daubert Standard, it no longer serves as the sole determining criterion (Fournier, 2016).

Overall, these guidelines offer a more balanced and evidence-based approach to evaluating forensic testimony, promoting the use of scientifically validated methods in courtrooms.

### **Rationale and Hypothesis**

Much of the existing research on ballistic trauma (Berryman, 2019; Hart, 2005; Humphrey et al. 2017; Ross 1996; Smith et al. 1987) has focused predominantly on GSW affecting the cranium and chest. Among long bones, the tibia is one of the most commonly fractured bones in gunshot incidents, along with the femur. Notably, fractures of the tibial diaphysis occur most frequently (Dougherty, 2009).

The present study examined the distinct characteristics and frequencies of ballistic trauma patterns in long bones, specifically using two common types of ammunition often encountered in firearm-related cases. Previous research by Henwood et al. (2019) demonstrated that bones typically fail biomechanically upon high-velocity impact, leading to minimal deformation of fragments. This phenomenon allows for the reassembly of bones and the analysis of entry wounds.

It was hypothesized that a statistically significant difference would exist in the occurrence of fragmentation and other ballistic trauma characteristics between 9 mm and 5.56 mm ammunition. The 5.56 mm rounds were discharged from an M4 rifle equipped with an 11.5-inch barrel, producing a muzzle velocity of approximately 2970 feet per second (FPS). Due to this higher velocity, it was anticipated that tibiae impacted by 5.56 mm ammunition would exhibit a greater degree of fragmentation and obscure fracture patterns. Conversely, fragmentation patterns associated with 9 mm ammunition were

expected to be more discernible, given the lower energy transfer and smaller caliber, allowing easier classification of fractures patterns including drill-hole, impaction, and false butterfly.

## **PREVIOUS RESEARCH**

### **Ballistic Fracture Patterns**

When a bone is impacted by a projectile, the way it fractures can be influenced by both intrinsic and extrinsic factors (Berryman et al. 2013). Intrinsic factors relate to the presence of soft tissue (Cohen et al. 2017), as well as the bone's own characteristics, such as its structural properties, mineral composition, age, nutrition, any present diseases, and its overall shape (Berryman et al. 2013; Wheatley 2008). Extrinsic factors involve elements like the bullet's design and composition, its caliber and velocity, the distance from which it was fired, any obstacles it may have struck along the way, and the angle of impact (Berryman et al. 2013; Berryman and Gunther 2000).

Gunshot injuries to long bones generally fall into three main categories: drill-hole, impaction, and false butterfly fractures (Smith and Wheatley 1984). Drill-hole fractures typically present as clean entry holes with internal beveling, exit wounds with greater fragmentation, and more likely to occur with lower velocity impacts (Huelke et al. 1967; Rose et al. 1988; Symes et al. 2012; Veenstra et al. 2022).

Impaction fractures, in contrast, happen when the projectile does not penetrate the bone. The projectile creates a depression or dislodges a piece of the outer cortical bone (Smith and Wheatley, 1984). False butterfly fractures are characterized by linear fracture lines radiating outward from the entry wound.

### **Model for Ballistic Trauma**

Ballistic experimentation normally must simulate human tissues using nonhuman animal analogs or synthetic materials. Conducting studies with postmortem human

subjects is uncommon due to the difficulty of obtaining tissue and the legal and ethical considerations involved (Caister et al. 2020). Researchers frequently must turn to substitutes like ballistic gelatin, nonhuman animal tissue, or a combination of both. For a model to be effective, it should closely replicate the energy dispersion and fracture mechanics of human bone, even though microstructural differences may remain (Schwab et al. 2023).

The present study utilized white-tailed deer (*Odocoileus virginianus*) tibiae instead of synthetic models, such as Synbone and Sawbone, which are medical human analogs designed to mimic bone, due to the greater similarity in fracture behavior between deer and human bone (Kieser et al. 2014). Research by Henwood and Appleby (2020) and Schwab et al. (2023) demonstrated that synthetic models tend to fracture in ways that differ significantly from human bone, while deer bone offers a closer comparison.

Schwab et al. (2023) evaluated the differences between Synbone models, human femora and humeri, and deer (*Cervus elaphus*) femora. After embedding both in ballistic gelatin to simulate soft tissue, they shot them with 9 mm bullets. While neither deer femora nor Synbone models perfectly matched the fracture patterns of human bone, the Synbone models were statistically more dissimilar. Similarly, Henwood and Appleby (2020) investigated how Synbone models compared to pig femora when exposed to various types of ammunition. Their findings indicated that Synbone should not be relied upon for accurate entry wound analysis or crack propagation studies. Research by Bir et al. (2016) further supported these conclusions, observing that both Sawbone and Synbone

models failed to replicate the fracture patterns seen in human bone when subjected to ballistic trauma. While synthetic models may perform well under slow-loading forces, their response to high-speed projectile forces produces unnaturally uniform fracture patterns.

When selecting an animal model for ballistic research, a species' size, morphology, and physiology are essential considerations (Muschler et al. 2010). One major distinction between adult human bone and nonhuman bone is the presence of plexiform bone, which consists of woven and lamellar layers. Though rarely found in adult humans, plexiform bone is present in young individuals and healing fracture sites (Porto et al. 2023). Over time, Haversian bone replaces plexiform tissue in both deer and humans. Despite differences in Haversian canal size and density, studies by Hillier and Bell (2007) confirmed that adult deer (*Odocoileus virginianus*) and human long bones share similar characteristics. Lyman (2014) and Kreutzer (1992) also reported comparable mineral densities between deer (*Odocoileus virginianus*) and human tibiae at various anatomical markers.

Ballistic gelatin has been utilized as a human soft tissue analog for decades, including a study by Fackler et al. (1984) to assess the wounding potential of an AK-74 assault rifle. With concentrations of 10% or 20% gelatin by mass, it accurately simulates human muscle tissue (Jussila et al. 2005). In medical research, ballistic gelatin has proven useful for biomechanical testing involving bending, pressure, shearing, and fall simulations (Biehl 2019). It has even been applied in exoskeleton research to replicate soft tissue deformation (Barrutia et al. 2023). In addition, ballistic gelatin demonstrates a

reliable ability to replicate projectile penetration depth and permanent tissue damage in both living and cadaveric tissue (Carr et al. 2018).

Some studies also highlighted the advantages of ballistic gelatin for data collection over nonhuman animal tissue. Widyastuti et al. (2023) examined frangible bullets and noted that extracting data from ballistic gelatin was considerably easier. Similarly, researchers like Nguyen et al. (2018) and Swain et al. (2014) charted a linear relationship between projectile penetration strength and velocity using gelatin. Watson et al. (2023) studied the impact of hollow-point ammunition on pig femora, encasing some in ballistic gelatin to simulate the posterior aspect of the human tibia or femur. Others were left un-encased to mimic the anterior tibia, where soft tissue is minimal. Watson et al. (2023) concluded that ballistic gelatin did not significantly alter bone failure mechanisms, supporting its continued use in realistic ballistic simulations.

## **METHODS**

### **Materials**

The present experiment was performed using white-tailed deer tibiae (n = 50) which were acquired commercially in December 2024. The deer tibiae were obtained pre-separated from the body and mostly defleshed. Any distal femur or proximal calcaneus portions that remained attached were removed by sawing, and the bones were immediately placed into a freezer for preservation until needed. The ballistic gelatin was obtained from Custom Collagen Incorporated, and the brand of gelatin chosen was Vyse® Professional Grade Ballistic Gelatin, as it is commonly used by law enforcement due to its ability to replicate human tissue (Ballistic Gelatin 2022).

Due to the range of deer tibiae sizes, plastic molds with the dimensions of 14  $\frac{3}{4}$  in. x 10  $\frac{1}{8}$  in. x 5  $\frac{5}{8}$  in. were used to accommodate the lengths of the largest ones. Each mold contained two deer tibiae separated by a thick aluminum and cardboard barrier to create two sections that could be shot individually. The total depth of the ballistic gelatin was 10 cm, with the anterior aspect of the tibiae being suspended approximately 5 cm below the surface (Figure 1). The gelatin blocks were created using a 90% water and 10% gelatin powder ratio.

To allow proper setting time prior to the shooting portion of the experiment, the deer tibiae in gelatin were prepared 2 days in advance and stored in a walk-in cooler set to 40°F at Boston University School of Medicine. The gelatin blocks must remain cold to maintain their structural integrity. The gelatin blocks have a working time of a few hours outside of the cooler, and prolonged exposure to heat will cause the gelatin to melt.

The shooting aspect of this experiment was carried out at the FBI Shooting Range in Fort Devens, Massachusetts. The ammunition utilized consisted of 135-grain 9 mm jacketed hollow point (JHP) bullets fired from a Glock 19 handgun with a muzzle velocity of 1070 FPS and 63-grain 5.56 x 45 mm bullets fired from an M4 rifle with an 11.5-inch barrel and a muzzle velocity of 2970 FPS. The ballistic gelatin blocks were kept in their plastic containers to maintain stability and propped up on a four-foot-tall plastic barrier in front of a dirt mound and shot from a distance of three yards. The sample was split in half, 25 shot with 9 mm ammunition and 25 shot with 5.56 mm ammunition. Each bone was impacted only once and then subsequently removed from the gelatin along with any bone fragments within the gelatin and placed into individually labeled bags. To avoid contamination, any fragments blown out the back of the molds into the mound were not collected, as it was impossible to determine which tibiae they originated from.

### **Data Collection and Statistics**

Bone marrow was removed with a metal scoop prior to maceration, and any remaining ballistic gelatin and soft tissue were scraped off. The bones were then placed into fine mesh bags and added to a slow cooker containing a water solution of 10 mL Biz® and 10 mL Dawn® Degreaser per liter of water. This solution was set to 175° F (79° C), and the bones were left to macerate for 12 hours. The tibiae were then removed from this solution, and any remaining adhering soft tissue was removed. Another solution of only 10 mL Dawn® Degreaser per liter of water set to 175° F (79° C) was made for further degreasing for another 36 hours. Once cleaned, the number of fragments  $\geq 2$  mm

in maximum length for each tibia were counted, and then the bones were reconstructed with Duco® cement and examined for the fracture patterns described above (drill-hole, impaction, and false butterfly). It was expected that the fractures would be comminuted, meaning that the fractures were complete and resulted in greater than two fragments (Galloway 1999). Drill-hole fractures, characterized by a clear, circular entry defect and a larger, more fragmented exit wound, were identified using criteria established by Huelke et al. (1967). False butterfly fractures, resembling those seen in blunt force trauma, were distinguished by four radiating oblique fractures forming a V-shape at the point of impact (Martrille and Symes 2019; Schwab et al. 2023). Impaction fractures occurred when the bullet caused a small depression without penetrating the bone (Smith and Wheatley 1984).

Additional characteristics of the GSW were documented: (1) entry wound shape, (2) bullet wipe presence, (3) stepped breakout, (4) diaphysis splitting, and (5) internal or (6) external beveling. Entry wound shapes were noted if a distinct form, such as round or square, was visible. Since the force of the gunshots could cause bone fragments to scatter or be destroyed, only partial reconstructions were possible in multiple cases. When intact, entry wound diameters were measured using digital calipers. Bullet wipe, visible as a dark stain around the entry wound, indicated residue from the bullet's surface, including metallic elements, soot, and lubricant (Pircher et al. 2019). Stepped breakout was identified by layered, similarly sized transverse fragments surrounding an exit wound. Splitting was marked when fracture lines extended from the impact point toward the epiphysis, causing a longitudinal split. Internal beveling appeared as a funnel-shaped

margin at the entry wound, while external beveling was similarly assessed (Lew et al. 2005).

Statistical analyses were performed utilizing IBM SPSS Statistics (Version 29.0.2.0). A Kolmogorov-Smirnov test was run to determine whether the number of fragments for each ammunition type followed a normal distribution pattern. A Mann-Whitney U-test was applied to determine if there was a significant difference in the number of fragments created by the two ammunition types. In addition, a Chi-square test was run for each GSW characteristic against the ammunition types to determine if there was a relationship between the two variables. The alpha level for statistical significance was set at 0.05.

## RESULTS

All the samples were markedly comminuted (Galloway 1999), with 25 to 95 fragments each. The 9 mm sample produced a range of 25 to 70 fragments, averaging  $48.2 \pm 12.9$  fragments, and the 5.56 mm sample produced a range of 36 to 95 fragments, averaging  $63.2 \pm 16.9$ . A Kolmogorov-Smirnov test determined that the number of fragments for each ammunition type followed a normal distribution pattern with (DF(25) = 0.139,  $p = 0.200$  for 9 mm; DF(25) = 0.090,  $p = 0.200$  for 5.56). A Mann-Whitney U-test indicated that 5.56 mm ammunition produced significantly more fragments than the 9 mm ( $p = 0.002$ ), with mean ranks of 19.10 and 31.90, respectively. Difficulty occurred when reconstructing the tibiae impacted with the 5.56 mm ammunition due to the loss of fragments and heavily comminuted nature of the defects (Figure 2).

A Chi-square test of independence assessed the relationship for each characteristic against the ammunition types. Internal beveling was observed in 64% (16/25) of the 9 mm sample compared to 8% (2/25) of the 5.56 mm sample. While the entry wounds of the 5.56 mm sample could not be fully reconstructed for further analysis, internal beveling was present on the tips of the V-shaped fragments toward the point of impact. The presence of internal beveling was significantly associated with 9 mm ammunition ( $\chi^2(1) = 17.014$ ,  $p = < 0.001$ ).

Clear entry wound shape were observed in 32% (8/25) of the 9 mm sample, contrasting the 5.56 mm sample which had no clear entry wound shapes. This association was statistically significant ( $\chi^2(1) = 9.524$ ,  $p = 0.002$ ), indicating that a discernable entry wound shape was more likely to occur in the 9 mm sample. Among the measurable entry

wounds ( $n = 6$ ) of the 9 mm sample, the diameters had a range of 14.2 mm to 18.4 mm, averaging  $15.6 \pm 1.6$  mm.

Bullet wipe was observed in 52% (13/25) of the 9 mm sample (Figure 3) and 16% (4/25) of the 5.56 mm sample. Due to the heavy fragmentation of the 5.56 mm sample, instances of bullet wipe were useful in determining the entry wound location. The presence of bullet wipe was significantly associated with 9 mm ammunition ( $\chi^2(1) = 7.219$ ,  $p = 0.007$ ), possibly in part due to the difficulty in reconstruction of the 5.56 mm wounds.

Stepped breakout was observed in 68% (17/25) of the 9 mm sample and 44% (11/25) of the 5.56 mm sample (Figure 4). Fragments were between 5-10 mm in size and rectangular in shape, giving a stacked brick-like appearance to the diaphysis. A statistically significant association was not seen between the presence of stepped breakout and ammunition type ( $\chi^2(1) = 1.299$ ,  $p = 0.254$ ).

Linear fracture patterns caused by the 5.56 mm ammunition extended along the diaphysis from the impact site, reaching the epiphysis and causing parallel fractures that split the diaphysis in half (Figures 5 and 6). Sections of the diaphysis were completely split in 32% (8/25) of the 5.56 mm sample, compared to only one instance of a diaphysis splitting in the 9 mm sample. The presence of diaphysis splitting was significantly associated with 5.56 mm ammunition ( $\chi^2(1) = 6.640$ ,  $p = 0.010$ ).

There were no instances where external beveling was observed in either sample. While many of the fracture patterns were highly irregular and could not be classified into drill-hole, impaction, or false butterfly fractures, false butterfly fractures were evident in

48% (12/25) of the 9 mm sample (Figures 7 and 8), as well as one instance (1/25) observed in the 5.56 mm sample. The false butterfly fracture pattern was significantly associated with 9 mm ammunition ( $\chi^2(1) = 12.578, p = < 0.001$ ).

## DISCUSSION

This study evaluated three primary categories of fracture patterns resulting from ballistic trauma: drill-hole, impaction, and false butterfly fractures. Although circular entry wounds were occasionally noted in the 9 mm sample, definitive drill-hole fractures were not observed. Furthermore, no entry wounds were observed for the 5.56mm sample. This is consistent with findings by Huelke et al. (1967), Rose et al. (1988), Symes et al. (2012), and Veenstra et al. (2022), who documented that drill-hole fractures are more typically associated with lower-velocity projectiles and shorter firing distances. In the current study, both ammunition types (9 mm and 5.56 mm) had relatively high muzzle velocities (1070 FPS and 2970 FPS, respectively), were fired from a distance of 3 yards, and impacted targets through a 5 cm layer of ballistic gelatin. These conditions likely contributed to the absence of classic drill-hole morphology, as the high energy transfer and intermediate target medium may have altered the resulting trauma patterns. Likewise, impact fractures, which only leave a depression on the surface of the target at the point of impact (Smith and Wheatley 1984), were not observed in any of the samples, as all projectiles fully penetrated the targets. False butterfly fractures, however, were prominently observed, especially in the 9 mm sample.

Schwab et al. (2023) conducted a comparable ballistic trauma study on the fragmentation of long bones from projectile impact, with a focus on comparing the behaviors between human long bones, Synbone models, and deer (*Cervus elaphus*) femora. All specimens were embedded in ballistic gelatin, with the target side 2 cm below the surface of the gelatin and impacted with 9 mm Luger full metal jacket (FMJ)

projectiles with an impact velocity of 360 m/s (~1181 FPS) (Schwab et al. 2023). Interestingly, Schwab et al. (2023) encountered a similar issue to the present study with reconstruction pertaining to the deer bone, noting that the deer femora in their study were heavily fragmented, hindering shaft reassembly, and allowing only partial reconstructions of the entry and exit wounds. In contrast, Schwab et al. (2023) did not encounter this reconstruction issue with the human long bones or Synbone samples, which were able to be fully reconstructed facilitating complete evaluation of wound characteristics. Despite reconstruction challenges, the use of deer bones remains a scientifically supported and statically validated methodology for studying ballistic trauma with findings that can be reasonably extrapolated to trauma in human long bones (Kieser et al. 2014).

Both the present study and Schwab et al. (2023) observed and analyzed the following characteristics using a Chi-square test of independence to assess fracture features: entry hole, bullet wipe, internal beveling, and external beveling. They also documented the vertical diameter of their entry wounds. Schwab et al. (2023) observed a round entry hole in 100% of human femora ( $n = 7$ ), 100% of human humeri ( $n = 7$ ), and 0% of the deer femora ( $n = 4$ ) ( $< 0.001$ ), while the present study observed 32% in the 9 mm sample, and 0% in the 5.56 mm sample. In their observations of bullet wipe, Schwab et al. (2023) had no occurrences in any of their human or deer samples, only finding bullet wipe in 100% of their Synbone sample. This result differed from the present study which observed bullet wipe in 52% of the 9 mm sample and 16% of the 5.56 mm sample of deer tibiae. Schwab et al. (2023) found internal beveling in 100% of their samples, compared to the present study which found internal beveling in 64% of the 9 mm sample

and 8% of the 5.56 mm sample. Interestingly, the most prominent difference between the two studies was the presence of external beveling observed in 100% of the human and deer samples for Schwab et al. (2023) and in 0% of both the 9 mm and 5.56 mm samples of the present study. Due to the heavy fragmentation of the deer femora, entry wound diameter was not measured by Schwab et al. (2023) but was documented for the present study and used for comparison. Schwab et al. (2023) recorded entry diameters of 9–11.5 mm (mean =  $10.4 \pm 1$  mm) in human femora and 9–11 mm (mean =  $10 \pm 0.7$  mm) in humeri. In contrast, the present study measured larger diameters ranging from 14.2 mm to 18.4 mm (mean =  $15.6 \pm 1.6$  mm).

Differences observed between the present study and the study performed by Schwab et al. (2023) could be attributed to several variables. Schwab et al. (2023) used a 9 mm FMJ bullet, while the present study used a 9 mm JHP bullet. The present study had an increase of 3 cm in gelatin depth to target and an increase of approximately one meter in firing distance. Consequently, the larger wound profiles observed in the present study may result from the use of 9 mm JHP rounds, which are designed to expand, as well as greater gelatin depth and a longer firing distance, both of which may influence projectile behavior (e.g., yaw, deformation) upon impact. Despite the differences in ballistic characteristics, Schwab et al. (2023) study noted the prevalence of stellate (false butterfly fractures) occurring in all samples which aligns with the prevalence of false butterfly fractures observed in the 9 mm sample of the present study.

Wound diameter also varied notably between the studies. Schwab et al. (2023) recorded entry diameters of 9–11.5 mm (mean =  $10.4 \pm 1$  mm) in human femora and 9–

11 mm (mean =  $10 \pm 0.7$  mm) in humeri. In contrast, the present study measured larger diameters ranging from 14.2 mm to 18.4 mm (mean =  $15.6 \pm 1.6$  mm). The larger wound profiles observed here may result from the use of 9 mm JHP rounds, which are designed to expand, as well as greater gelatin depth and a longer firing distance, both of which may influence projectile behavior upon impact.

Martrille and Symes (2019) critically assessed the applicability of cranial ballistic trauma models to postcranial long bones. Their reevaluation of femoral gunshot wounds in autopsy cases revealed false butterfly fractures without clear exit wounds in several cases. For instance, in cases involving .38 Special and 7.62 x 39 mm rounds, extensive radiating fractures disrupted the bone architecture so significantly that the bullet failed to produce a discrete exit wound. This phenomenon was also observed in the present study, where exit wounds were often obscured or unidentifiable due to severe fragmentation, particularly in the 5.56 mm group.

Langley (2007) highlighted how the tubular shape of long bones, coupled with their cortical and woven bone composition, often leads to the diaphysis ‘exploding’ upon impact. This fragmentation makes it difficult to identify exit wounds clearly, as the fractures tend to propagate more rapidly than the projectile itself. Once reconstructed, the bones in the present study exhibited well-defined entrance wounds but lacked similarly distinct exit wounds (Figure 9), consistent with Langley’s findings. Additionally, Quatrehomme and İşcan (1999) noted that exit wounds are generally larger and more irregular than entry wounds, which was evident in the reconstructed samples of the present study.

The present study aimed to evaluate the relationship between wound diameter and ammunition caliber. Henwood et al. (2019) compared entry wound diameters in pig femora from .22 caliber, .38 caliber, and 9 mm bullets using a Kruskal-Wallis test. Significant differences between the median entry wound diameters were observed between a 0.22 caliber and 0.38 caliber, as well as a 0.22 caliber and a 9 mm entry wound (0.007). However, there was no significant difference between .38 caliber and 9 mm projectiles. Due to their similar caliber size, a pairwise comparison *post hoc* test determined that there were no statistical differences between the median diameter sizes of the entry wounds (0.734), reinforcing the challenge of differentiating closely sized calibers. In a forensic context, this variability supports a more general classification of ammunition such as ‘small’ or ‘large’ caliber particularly when assessing wound diameter in fractured remains.

## CONCLUSIONS

The present study investigated the characteristics, fragmentation, and fracture patterns of long bones impacted by 9 mm and 5.56 mm ammunition using deer tibiae as a human analog. A statistically significant difference was observed in the occurrence of fragmentation and other ballistic trauma characteristics between 9 mm and 5.56 mm ammunition. The 5.56 mm rounds were discharged from an M4 rifle equipped with an 11.5-inch barrel, producing a muzzle velocity of approximately 2970 FPS. Due to the higher velocity, the tibiae impacted by 5.56 mm ammunition exhibited a greater degree of fragmentation and obscured fracture patterns. Conversely, fragmentation patterns associated with 9 mm ammunition were more discernible, given the lower energy transfer and smaller caliber, allowing easier classification of fracture patterns including false butterfly. While it was anticipated that both drill-hole and impact fractures would be observed, only false butterfly fractures were present. These results support the hypothesis that projectile caliber and muzzle velocity influence the expression of specific fracture patterns, wound morphology, and ballistic characteristics in long bones.

Although statistical differences were evident in fracture characteristics, the most pronounced was the extent of fragmentation. In practice, this level of bone fragmentation and the presence of irregular fracture patterns in the 5.56 mm sample may be a strong indicator in the identification of ammunition caliber. In addition, the formation of false butterfly fractures in the 9 mm sample, along with internal beveling and bullet wipe, served as reliable distinguishing characteristics in this study. Stepped breakout fractures

did not, however, show a statistically significant difference, suggesting they may not be a reliable indicator for ammunition type in forensic interpretations.

The use of deer tibiae, despite reconstruction challenges, remains a scientifically supported and statistically validated model for simulating ballistic trauma in human long bones (Schwab et al., 2023). Though anatomical and structural differences exist, the extrapolation of findings to human forensic cases is justifiable, particularly in studies focused on fracture classification and general ballistic behavior.

Overall, this study supports the hypothesis that 5.56 mm ammunition produces more extensive fragmentation and yields distinct fracture patterns compared to 9 mm rounds. These findings contribute to the forensic interpretation of long bone ballistic trauma, especially in cases where skull trauma is not present. Future research should include direct velocity measurements at impact, testing additional ammunition types, and expanding biological models to further validate and standardize methodologies. Continued refinement of ballistic trauma analysis is essential for enhancing forensic reliability and ensuring alignment with evidentiary standards such as those outlined in *Daubert v. Merrell Dow Pharmaceuticals* (Dirkmaat et al. 2008).



**Figure 1. Two deer tibiae are embedded in 10 cm of ballistic gelatin. The anterior aspects are approximately 5 cm below the surface. There is an aluminum divider between the two tibiae, so they can each be impacted separately.**



**Figure 2. Anterior aspect of tibia impacted by 5.56 mm ammunition. The entry and exit wounds are heavily comminuted, irregular, and largely indistinguishable from each other. Long oblique fracture lines run along the diaphysis toward the far proximal and distal extremities. The scale is in cm.**

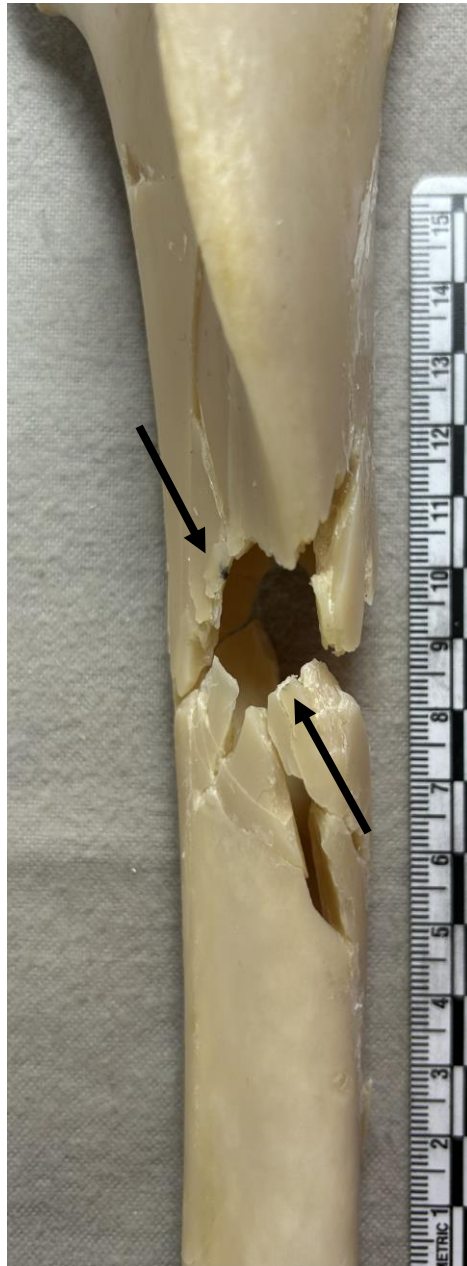


**Figure 3. Anterior aspect of tibia impacted by 9 mm ammunition. The entry wound is round with radiating and concentric fractures. Internal beveling is present. Bullet wipe (arrows) is evident along the margins of the entry wound. The scale is in cm.**

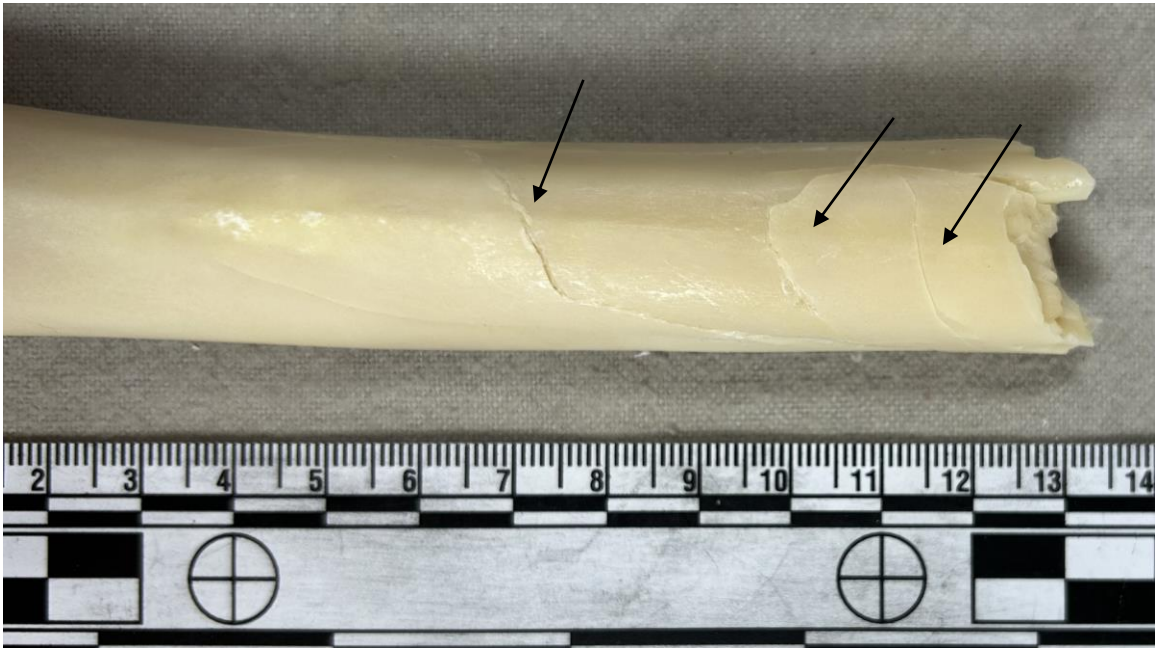


**Figure 4. Postero-distal portion of tibia impacted by 5.56 mm ammunition. Layered concentric fractures (arrows) on the posterior surface are created by a stepped breakout fracture pattern. Stepped breakout pattern is distinguishable by the similar shaped fragments. The scale is in cm.**

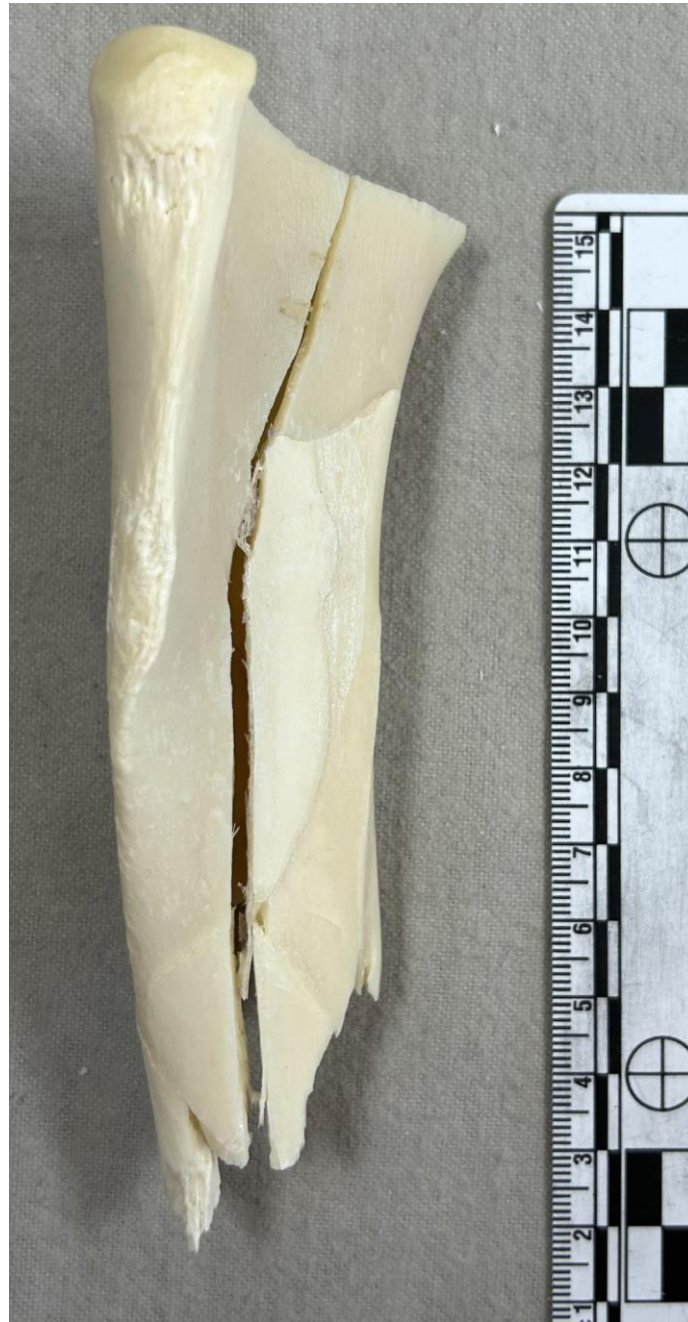


**Figure 5. Antero-proximal portion of tibia impacted by 5.56 mm ammunition. The impact created a long radiating fracture that split the diaphysis in half. The scale is in cm.**



**Figure 6. Distal portion of tibia impacted by 5.56 mm ammunition. A long, oblique radiating fracture line runs distally down the diaphysis. The scale is in cm.**



**Figure 7. Anterior aspect of tibia impacted by 9 mm ammunition. The entry wound is rounded with radiating linear fractures. Pattern formed by impact is a false butterfly fracture. The scale is in cm.**



**Figure 8. Anterior aspect of tibia impacted with 9 mm ammunition. The entry wound is round, with internal beveling and small specks of bullet wipe along the margins. A false butterfly fracture pattern is created by the four prominent fracture lines radiating from the entry wound. The scale is in cm.**



**Figure 9. Posterior aspect of tibia impact by 9 mm ammunition. Entry wound is round and exit wound is irregular and more comminuted. Fracture margins are jagged and no external beveling could be observed around the exit wound. Posterior aspect shows stepped breakout consisting of radiating and concentric fractures. The scale is in cm.**

**Table 1. Fragmentation of 9 mm and 5.56 mm samples.**

	<b>9 mm</b>	<b>5.56 mm</b>
<b>Minimum Number of Fragments</b>	25	36
<b>Maximum Number of Fragments</b>	70	95
<b>Mean</b>	48.2	63.2
<b>Standard Deviation</b>	12.9	16.9

**Table 2. Observed characteristics of ballistic trauma based upon ammunition.**

	<b>9 mm</b>	<b>5.56 Caliber</b>	<b><i>p</i> Value</b>
<b>Entry wound visible</b>	8	0	0.002
<b>Internal beveling</b>	16	2	< 0.001
<b>External beveling</b>	0	0	-
<b>Bullet wipe</b>	13	4	0.007
<b>Stepped breakage</b>	17	11	0.254
<b>Split diaphysis</b>	1	6	0.010
<b>Butterfly fracture</b>	12	1	< 0.001

**BIBLIOGRAPHY**

- Ballistic gelatin: Learn how our ballistics gelatin mix helps law enforcement at custom collagen. (2022). Retrieved from <https://customcollagen.com/ballistic-gelatin/>.
- Barrutia W. S., Bratt, J., Ferris, D.P. (2023) A Human Lower Limb Mechanical Phantom for the Testing of Knee Exoskeletons, *IEEE Transactions on Neural Systems and Rehabilitation Engineering*, 31, 2497-2506.
- Berryman, H. E. (2019). A systematic approach to the interpretation of gunshot wound trauma to the cranium. *Forensic Science International*, 301, 306–317.  
<https://doi.org/10.1016/j.forsciint.2019.05.019>
- Berryman, H. E., and W. M. Gunther (2000) Keyhole defect production in tubular bone. *Journal of Forensic Sciences* 45(2):483-487.
- Berryman, H. E., N. R. Shirley, and A. K. Lanfear (2013) Basic gunshot interpretation in forensic anthropology. In *Forensic Anthropology: An Introduction* ed. by M. A. Tersigni-Tarrant and N. R. Shirley, pp. 291-306. CRC Press, Boca Raton, FL.
- Biehl (2019) 23rd Surgical Research Days. *European Surgical Research*; 60 (3-4): 117–178.
- Bir, C., Andrecovich, C., DeMaio, M., and Dougherty, P. J. (2016). Evaluation of bone surrogates for indirect and direct ballistic fractures. *Forensic Science International*, 261, 1–7.
- Brownlee, C. (2023). Gun Violence by the Numbers in 2023. In: *The Trace*
- Caister, A. J., Carr, D. J., Campbell, P. D., Brock, F., and Breeze, J. (2020) The ballistic performance of bone when impacted by fragments. *International Journal of Legal Medicine*, 134(4): 1387–1393.

- Carr, D.J., Stevenson, T. and Mahoney, P.F. (2018) The use of gelatine in wound ballistics research. *International Journal of Legal Medicine*, 132, 1659–1664.
- Cheng, E. K., and Yoon, A. H. (2005). Does Frye or Daubert Matter? A Study of Scientific Admissibility Standards. *Virginia Law Review*, 91(2), 471–513.
- Cohen, Kugel, C., May, H., Medlej, B., Stein, D., Slon, V., Brosh, T., and Hershkovitz, I. (2017) The effect of impact tool geometry and soft material covering on long bone fracture patterns in children. *International Journal of Legal Medicine*, 131(4), 1011–1021.
- Dirkmaat, D. C., Cabo, L. L., Ousley, S. D., and Symes, S. A. (2008). New perspectives in forensic anthropology. *American Journal of Physical Anthropology*, 137(S47), 33–52. <https://doi.org/10.1002/ajpa.20948>
- Dougherty PJ, Vaidya R, Silverton CD, Bartlett C, Najibi S. (2009) Joint and long-bone gunshot injuries. *Journal of Bone and Joint Surgery*, 91(4), 980-997.
- Fackler, Martin L. M.D.; Surinchak, John S. M.A.; Malinowski, John A. B.S.; Bowen, Robert E. (1984) Wounding Potential of the Russian AK-74 Assault Rifle. *The Journal of Trauma: Injury, Infection, and Critical Care*, 24(3): 263-266.
- Fienberg, S. E., Krislov, S. H., and Straf, M. L. (1995). UNDERSTANDING AND EVALUATING STATISTICAL EVIDENCE IN LITIGATION. *Jurimetrics*, 36(1), 1–32.
- Flieger, Kölzer, S. C., Plenzig, S., Heinbuch, S., Kettner, M., Ramsthaler, F., and Verhoff, M. A. (2016) Bony injuries in homicide cases (1994–2014). A retrospective study. *International Journal of Legal Medicine*, 130(5), 1401–1408.
- Fournier, Lisa R. (2016) The Daubert Guidelines: Usefulness, Utilization, and Suggestions for Improving Quality Control. *Journal of Applied Research in Memory and Cognition*, 5(3): 308-313.

- Galloway, A. (1999) The biomechanics of fracture production. In: Galloway, A., editor. Broken bones: Anthropological analysis of blunt force trauma. Springfield, IL: Charles C Thomas. Pp. 35-62.
- Hart, G. (2005). Fracture Pattern Interpretation in the Skull: Differentiating Blunt Force from Ballistics Trauma Using Concentric Fractures. *Journal of Forensic Sciences*, 50(6), JFS2004219-6. <https://doi.org/10.1520/JFS2004219>
- Hawes, Chancellor, K. E., Rogers, W. R., and Ledford, J. A. (2016) Fatal Firearm Injuries in Tennessee: A Comparison Study of Tennessee's Two Most Populous Counties 2009-2012. *Journal of Forensic Sciences*, 61(3), 666–670.
- Henwood, B.J., Oost, T.S. and Fairgrieve, S.I. (2019) Bullet Caliber and Type Categorization from Gunshot Wounds in *Sus scrofa* (Linnaeus) Long Bone. *Journal of Forensic Sciences*, 64: 1139-1144.
- Henwood, B.J. and Appleby-Thomas, G. (2020) The suitability of Synbone® as a tissue analogue in ballistic impacts. *Journal of Materials Science*, 55, 3022–3033.
- Hillier, M.L., Bell, L.S. (2007) Differentiating human bone from animal bone: a review of histological methods. *Journal of Forensic Sciences*; 52(2):249–63.
- Huelke, Donald F., Buege, Lynn J., Harger, James H. (1967) Bone fractures produced by high velocity impacts†
- Humphrey, C., Kumaratilake, J., and Henneberg, M. (2017). Variability of characteristics of cranial projectile trauma in skeletal material. *Anthropologischer Anzeiger*, 74(4), 283–296. <https://doi.org/10.1127/anthranz/2017/0774>
- Jussila, J., Leppäniemi, A., Paronen, M., Kulomäki, E. (2005) Ballistic skin simulant. *Forensic Science International*, 150(1), 63-71.

- Kieser, D.C., Kanade, S., Waddell, N.J., Kieser, J.A., Theis, J.C., Swain, M.V. (2014) The deer femur-a morphological and biomechanical animal model of the human femur. *Bio-Medical Materials and Engineering*; 24(4):1693–703.
- Koper, CS. (2020) Assessing the potential to reduce deaths and injuries from mass shootings through restrictions on assault weapons and other high-capacity semiautomatic firearms. *Criminal Public Policy*, 19: 147–170.
- Kreutzer, L.A., (1992) Bison and deer bone mineral densities: Comparisons and implications for the interpretation of archaeological faunas. *Journal of Archaeological Science*, 19 (3): 271-294.
- Langley. (2007) An Anthropological Analysis of Gunshot Wounds to the Chest. *Journal of Forensic Sciences*, 52(3), 532–537.
- Lew, E., Dolinak, D., and Matshes, E. (2005) Chapter 7: Firearm Injuries. In: *Forensic Pathology Principles and Practice*. Pp. 162-200.
- Lyman, R.L. (2014) Bone density and bone attrition. In: Pokines, J.T., Symes, S.A., editors. *Manual of forensic taphonomy*. Boca Raton, FL: CRC Press; 51–72.
- Maiden, N. R., Hiss, J., Gips, H., Hoeherman, G., Levin, N., Kosachevsky, O., Vinokurov, A., Zelkowicz, A., Byard, R. W. (2016) An analysis of the characteristics of thoracic and abdominal injuries due to gunshot homicides in Israel. *Journal of Forensic Sciences*, 61(1), 87-92.
- Martrille, L., and Symes, S. A. (2019) Interpretation of long bones ballistic trauma. *Forensic Science International*, 302.
- Muschler, G.F., Raut, V.P., Patterson, T.E., Wenke, J.C., Hollinger, J.O. (2010) The design and use of animal models for translational research in bone tissue engineering and regenerative medicine. *Tissue Engineering*; 16(1):123–45.

- Nguyen, T., Tear, G. R., Masouros, S. D., Proud, W. G.; Fragment penetrating injury to long bones. AIP Conf. Proc. 3 July 2018.
- Pircher, R., Große Perdekamp, M., Mierdel, K., Pollak, S., Thierauf-Emberger, A., and Geisenberger, D. (2019). Bullet wipe on the uppermost textile layer of gunshot entrance sites: may it be absent due to pre-existing blood staining? *International Journal of Legal Medicine*, 133(5), 1437–1442.
- Porto, S., Flavel, A., Maggio, A., and Franklin, D. (2023). Differentiating human from non-human bone fragments through histomorphological assessment of remains from Camposanto cemetery, Italy. *Archaeometry*, 65(1), 213–229.
- Quatrehomme, G., and M. Y. İşçan (1999) Characteristics of gunshot wounds in the skull. *Journal of Forensic Sciences* 44(3):568-576.
- Rickman, J.M. and Smith, M.J. (2014) Scanning Electron Microscope Analysis of Gunshot Defects to Bone: An Underutilized Source of Information on Ballistic Trauma. *Journal of Forensic Sciences*, 59: 1473-1486.
- Ross, A. (1996). Caliber Estimation from Cranial Entrance Defect Measurements. *Journal of Forensic Sciences*, 41(4), 629–633. <https://doi.org/10.1520/JFS13966J>
- Rose, S. C., Fujisaki C. K., Moore, E.E. (1988) Incomplete fractures associated with penetrating trauma: etiology, appearance, and natural history. *The Journal of Trauma*, 28(1):106–9.
- Schwab, N., Jordana, X., Soler, J., Garrido, X., Brillas, P., Savio, A., Lavin, S., Ortega-Sanchez, M., and Galtés, I. (2023) Can Synbone® cylinders and deer femurs reproduce ballistic fracture patterns observed in human long bones? *Journal of Materials Science*, 58, 4970–4986.
- Sexton, K., Schwab, N., Galtés, I., Casas, A., Armentano, N., Brillas, P., Garrido, X., and Jordana, X. (2024). Osteonal Damage Patterns from Ballistic and Blunt Force Trauma in Human Long Bones. *Life (Basel, Switzerland)*, 14(2), 220-.

- Smith, O., Berryman, H., and Lahren, C. (1987). Cranial Fracture Patterns and Estimate of Direction from Low Velocity Gunshot Wounds. *Journal of Forensic Sciences*, 32(5), 1416–1421. <https://doi.org/10.1520/JFS11188J>
- Smith, Howard W. and Wheatley, Kenneth K. (1984) Biomechanics of Femur Fractures Secondary to Gunshot Wounds. *The Journal of Trauma: Injury, Infection, and Critical Care*, 24(11): 970-977.
- Su, Charles A., Nguyen, Mai P., O'Donnell, Jeffrey A., Vallier, Heather A. (2018) Outcomes of tibia shaft fractures caused by low energy gunshot wounds. *Injury*, 49, 1348-1352.
- Swain, M. V., Kieser, D. C., Shah, S., and Kieser, J. A. (2014). Projectile penetration into ballistic gelatin. *Journal of the Mechanical Behavior of Biomedical Materials*, 29, 385–392.
- Symes, S. A., L'Abbé, E. N., Chapman, E. N., Wolff, I., & Dirkmaat, D. C. (2012). Interpreting Traumatic Injury to Bone in Medicolegal Investigations. In *A Companion to Forensic Anthropology* (pp. 340–389). John Wiley & Sons, Ltd.
- Veenstra, A., Kerkhoff, W., Oostra, R.-J., and Galtés, I. (2022). Gunshot trauma in human long bones: towards practical diagnostic guidance for forensic anthropologists. *Forensic Science, Medicine, and Pathology*, 18(3), 359–367.
- Watson, KE, Henwood, BJ, Hewins, K, Roberts, A, Hazael, R. (2023) Ballistic impact of hollow-point ammunition on porcine bone. *Journal of Forensic Sciences*, 68: 1121–1132.
- Wheatley, B.P. (2008) Perimortem or postmortem bone fractures? An experimental study of fracture patterns in deer femora. *Journal of Forensic Sciences*, 53 (1):69–72.
- Widyastuti, Adhy Prihatmiko Wibowo, Bambang Pramujati, Denny Lesmana, Afrizal Aditya Pratama, Sugiarto Putra Wijaya (2023) Lagrangian approach embed with

discrete element method for extreme deformation study in frangible bullet designs  
fragmentation and penetration on viscoelastic ballistic gel. Heliyon 9(4).

**CURRICULUM VITAE**

